

# Theoretical Investigation of the Adsorption and Diffusion of Hydrogen on the Surface and in the Bulk of the Intermetallic Compound $Mg_2Ni$

A. A. Kuzubov<sup>a, b, c, \*</sup>, N. S. Eliseeva<sup>a</sup>, P. O. Krasnov<sup>b, c</sup>, A. V. Kuklin<sup>a</sup>,  
E. A. Kovaleva<sup>a</sup>, and A. S. Kholobina<sup>a</sup>

<sup>a</sup> Siberian Federal University, pr. Svobodnyi 79, Krasnoyarsk, 660041 Russia

\* e-mail: alexkuzubov@gmail.com

<sup>b</sup> Kirensky Institute of Physics, Siberian Branch of the Russian Academy of Sciences,  
Akademgorodok 50-38, Krasnoyarsk, 660036 Russia

<sup>c</sup> Siberian State Technological University, pr. Mira 82, Krasnoyarsk, 660049 Russia

Received April 22, 2014

**Abstract**—The intermetallic compound  $Mg_2Ni$  as a potential material for hydrogen storage has been investigated theoretically. The sorption and diffusion of a hydrogen atom in the bulk and on the surface of this material, as well as the step-by-step process of dissociative chemisorption of a  $H_2$  molecule on the surface, have been considered. The dependence of the sorption energy of atomic hydrogen on the structural characteristics of the intermetallic compound  $Mg_2Ni$  has been analyzed.

DOI: 10.1134/S1063783414100187

## 1. INTRODUCTION

With increasing environmental problems due to the use of fossil fuels, the transition to alternative energy sources is becoming ever more important. One of such sources is hydrogen. The prospect of using this source is associated with the fact that it is renewable, environmentally friendly, and contains a large amount of energy per unit mass. However, the main obstacle to the transition to hydrogen power engineering is the lack of materials for efficient hydrogen storage.

Of great importance for solving problems of hydrogen power engineering are hydrides of intermetallic compounds of the general formula  $A_mB_nH_x$ , where  $A_mB_n$  is a compound of two or more metals from the series of intermetallic hydrides, one of which ( $A$ ) forms a stable binary hydride and the other ( $B$ ) does not interact with hydrogen under normal conditions but is a catalyst for the dissociation of  $H_2$  molecules. Among different types of intermetallic hydrides, the most important in practice are the compounds  $AB_5$  ( $CaCu_5$  structure type),  $AB_2$  (Laves phase),  $AB$  ( $CsCl$  type structure), and  $A_2B$  ( $B_2Al$  structure type). The component  $A$  is a rare-earth metal or calcium in the first case, an element of the titanium subgroup in the second and third cases, and predominantly magnesium in the fourth case. The component  $B$  in all the above families is predominantly a transition metal (Fe, Co, Ni, V, Mn, or Cr) [1].

Under mild conditions, intermetallic hydrides are characterized by the hydrogen absorption/release

kinetics suitable for practical use and, therefore, are best suited for creating hydrogen storage systems [2, 3]. However, the practical implementation involves solving a number of problems, including an increase in the rate of hydrogen sorption–desorption processes and an increase in the cyclic stability of the adsorbent material. There are also required in-depth theoretical and experimental research in the field of physico-chemical properties of intermetallic compounds and the related hydrides.

Intermetallic compounds based on magnesium are the most promising materials for hydrogen storage owing to their relatively high hydrogen storage capacity, wide abundance of magnesium in the Earth's crust, and its low cost as compared to alternative materials [4]. Among all the known magnesium-based alloys, magnesium nickelide  $Mg_2Ni$  with a hexagonal crystal lattice can be easily synthesized. This intermetallic compound can also be formed upon evaporation of nickel on a magnesium plate or a magnesium particle. Magnesium nickelide easily and rapidly reacts with hydrogen to form the  $Mg_2NiH_4$  hydride [5, 6]. After the hydrogenation,  $Mg_2Ni$  undergoes a structural rearrangement and transforms into the  $Mg_2NiH_4$  hydride [7]. Under a pressure of 1 atm, this hydride transforms from the high-temperature cubic phase into the low-temperature monoclinic phase at the transition temperature ranging from 483 to 518 K [8–10].

Since a material absorbing hydrogen at low pressures and low temperatures is most suited for practical use of hydrogen adsorbents, the low-temperature

phase of  $\text{Mg}_2\text{NiH}_4$  has attracted the particular attention of researchers engaged in the field of hydrogen storage materials [11–14]. In particular, the thermodynamic, electronic, and optical properties of this phase were investigated by Myers et al. [11] using ab initio calculations. It was also found that the geometry of the  $\text{NiH}_4$  complex is close to a regular tetrahedron, which agrees with the neutron diffraction data [15]. Häussermann et al. [12] carried out ab initio density functional calculations of the structural stability of the low-temperature phases of  $\text{Mg}_2\text{NiH}_4$  and  $\text{Ba}_2\text{PdH}_4$ . The revealed difference between hydrogen bonding situations in these compounds was explained by the difference in the interaction forces of the  $\text{Ni}(\text{Pd})\text{--H}$  and  $\text{Mg}(\text{Ba})\text{--H}$  groups. The authors proposed the idea that the temperature of hydrogen desorption from  $\text{Mg}_2\text{NiH}_4$  can be decreased by introducing defects (for example, replacement of Mg atoms by Al atoms) in the vicinity of the tetrahedral complex  $\text{NiH}_4$ . Jasen et al. [13] also calculated the electronic structure and bonding of the low-temperature phase of  $\text{Mg}_2\text{NiH}_4$  in the local density approximation (LDA). It was shown that the hydrogen bond with nickel is stronger than that with magnesium, and the principal bonding interaction in the hydride is the  $\text{Ni } sp\text{--H } s$  interaction. Based on their density functional theory calculations of the hydrogenation reaction heat, the enthalpy of formation, and the energy required to remove the hydrogen atom, Zhang et al. [14] concluded that, during the hydrogenation of  $\text{Mg}_2\text{Ni}$ , the probability of the formation of the low-temperature phase of  $\text{Mg}_2\text{NiH}_4$  is higher than that of the high-temperature phase. Moreover, the idea was proposed that the removal of hydrogen at low temperatures from the low-temperature phase of  $\text{Mg}_2\text{NiH}_4$  with a high structural stability requires doping of the material with catalytic impurities that facilitate the sorption/desorption processes.

The results of the aforementioned works are mainly concerned with the thermodynamic aspects of the formation of the low-temperature phase of  $\text{Mg}_2\text{NiH}_4$  and desorption of  $\text{H}_2$  molecules from it. The kinetic features of these processes, which also determine the possibility of using the  $\text{Mg}_2\text{Ni}$  intermetallic compound as a hydrogen storage material, have not been considered. Therefore, the purpose of this work was to perform a theoretical study of the hydrogen sorption and diffusion in the bulk and on the surface of pure  $\text{Mg}_2\text{Ni}$ .

## 2. OBJECTS AND METHODS OF INVESTIGATION

In this work, we carried out the quantum-chemical simulation using the Vienna Ab Initio Simulation Package (VASP 5.3) [16–18] in terms of the density functional theory (DFT) [19, 20] with the plane wave basis set and the projector augmented wave (PAW) method [21, 22]. The calculations were performed in the generalized gradient approximation (GGA) for the

Perdew–Burke–Ernzerhof (PBE) exchange–correlation functional with the Grimme’s correction taking into account the van der Waals interaction [23]. The transition state and potential barriers to transition of the hydrogen atom inside the  $\text{Mg}_2\text{Ni}$  structure were found using the nudged elastic band (NEB) method [24, 25].

At the initial stage of the study, we simulated the hexagonal unit cell of  $\text{Mg}_2\text{Ni}$ . When optimizing the geometry of the unit cell for integration in the first Brillouin zone (1 BZ), this zone was automatically divided into a  $12 \times 12 \times 2$  Monkhorst–Pack  $k$ -point grid [26]. Further, in order to investigate the diffusion of the hydrogen atom in the bulk of  $\text{Mg}_2\text{Ni}$ , we constructed a supercell ( $\text{Mg}_{108}\text{Ni}_{54}$ ) consisting of  $3 \times 3 \times 1$  unit cells.

The sorption and diffusion of the hydrogen atom, as well as the sorption and dissociation of the hydrogen molecule, on the surface of the intermetallic compound were investigated by means of the simulation of a plate. The plate was constructed by the translation of the  $\text{Mg}_2\text{Ni}$  unit cell along the crystallographic direction [001]. In calculations with periodic boundary conditions, samples of the plate were separated by a vacuum gap of 15 Å. According to test calculations, this gap makes it possible to almost completely exclude the influence of the plate samples on one another. Then, we calculated several variants for the considered surface, which differed from each other by the displacement of the cut plane along the unit cell. In this case, both surfaces of the plate had identical ends. The most energetically favorable structure (with a surface energy difference of  $\sim 0.03 \text{ eV}/\text{Å}^2$ ) had the surface terminated by two magnesium layers. Based on the results of the test calculations, the surface interaction of the intermetallic compound with hydrogen was simulated using the  $\text{Mg}_{126}\text{Ni}_{54}$  plate consisting of  $3 \times 3$  unit cells with a thickness of 12.841 Å.

The geometry optimization of the structures of the supercell and the plate (because of their large dimensions) was carried out for  $2 \times 2 \times 2$  and  $2 \times 2 \times 1$   $k$ -point grids along each of the directions, respectively. In the calculations, the cut-off energy of the plane waves was 269.5 eV. The geometry optimization of the studied structures during the simulation was performed until the maximum forces acting on atoms reached 0.01 eV/Å.

In order to determine the most energetically favorable positions of the hydrogen atom in the bulk and on the surface of  $\text{Mg}_2\text{Ni}$ , as well as those of the hydrogen molecule on the surface of this compound, we calculated structures with its different locations. The formation energy of the compound per hydrogen atom was calculated according to the formula

$$E = E_{\text{Mg}_x\text{Ni}_y\text{H}_z} - E_{\text{Mg}_x\text{Ni}_y} - 0.5zE_{\text{H}_2}, \quad (1)$$

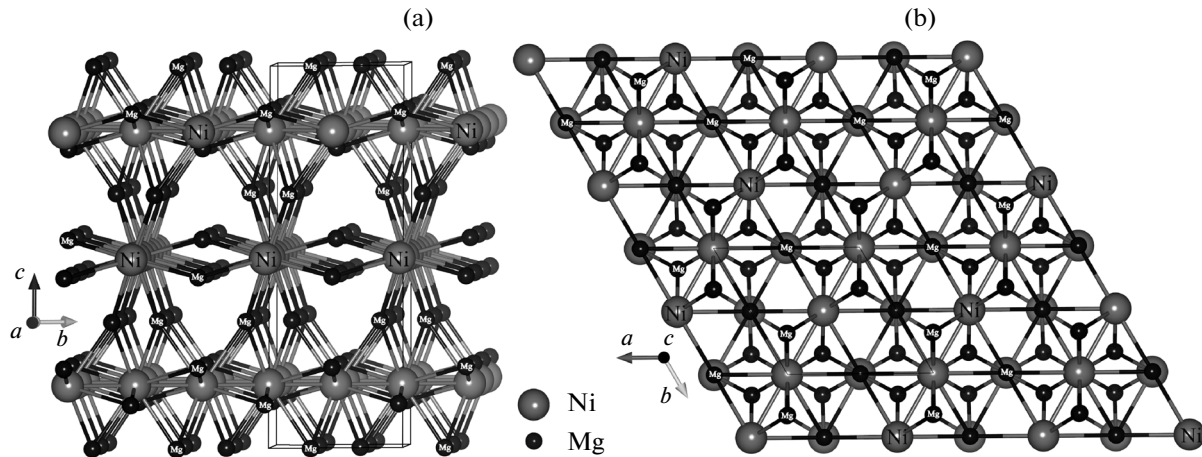


**Fig. 1.** Atomic structure of the  $\text{Mg}_2\text{Ni}$  intermetallic compound: (a) view from the  $[100]$  direction and (b) view from the  $[001]$  direction.

where  $E_{\text{Mg}_x\text{Ni}_y\text{H}_z}$ ,  $E_{\text{Mg}_x\text{Ni}_y}$ , and  $E_{\text{H}_2}$  are the total energy of the system with different numbers  $z$  of hydrogen atoms ( $z = 1, 2, 4$ ), the total energy of the supercell or plate of the  $\text{Mg}_2\text{Ni}$  intermetallic compound, and the total energy of the hydrogen molecule, respectively.

### 3. RESULTS AND DISCUSSION

The unit cell parameters of  $\text{Mg}_2\text{Ni}$ , which were obtained by the geometry optimization of the structure (Fig. 1), agree well with the experimental values (Table 1) [10]. The  $\text{Mg}_2\text{Ni}$  intermetallic compound has a structure consisting of chains of nickel atoms in the form of layers located parallel to the  $(110)$  plane. The distance between the chains within a layer is  $4.438 \text{ \AA}$ , the distance between the Ni atoms located in different layers is  $4.342 \text{ \AA}$ , and the distance between the Ni atoms within a chain is  $2.562 \text{ \AA}$ . The chains have the same direction within the layer and are rotated by  $60^\circ$  with respect to each other in the adjacent layers. Each Ni atom is surrounded by eight Mg atoms located at a distance of  $\sim 2.638 \text{ \AA}$  from it. All the magnesium atoms are bridging, because they are bonded simultaneously to two neighboring nickel atoms in the row.

The most energetically favorable hydrogen sorption positions in the bulk of  $\text{Mg}_2\text{Ni}$  are most likely located near the Ni atoms, as in the  $\text{Mg}_2\text{NiH}_4$  hydride. This assumption was checked using a  $3 \times 3 \times 1$  supercell of  $\text{Mg}_2\text{Ni}$  ( $\text{Mg}_{108}\text{Ni}_{54}$ ) by calculating the binding energy of H atoms in different positions (Fig. 2, Table 2). The obtained values allow us to conclude that, in the case of low concentrations, hydrogen will tend to occupy the most energetically favorable positions  $2_{\text{vol}}$  and  $3_{\text{vol}}$ . In these positions, the H atoms are bridging, because they are located at equal distances from two neighboring Ni atoms, which, in turn, enhances the

binding of atomic hydrogen. The positions  $2_{\text{vol}}$  and  $3_{\text{vol}}$  are closely located to each other in terms of the geometry of the complex but differ from each other by the positions of the H atoms with respect to one of the nearest neighbor atoms of magnesium and nickel from other atomic layers. In the  $2_{\text{vol}}$  position, hydrogen is located more closely to one of the Mg atoms surrounding the Ni atom, as compared to the  $3_{\text{vol}}$  configuration. This interaction can be responsible for the higher stability of the  $2_{\text{vol}}$  configuration. It should be noted that the filling of such positions around one nickel atom ( $2_{\text{vol}}$  and  $3_{\text{vol}}$ ) leads to the formation of the  $\text{NiH}_4$  complex with a tetrahedral configuration.

The Ni–H bond lengths in the low-temperature phase of  $\text{Mg}_2\text{NiH}_4$  lie in the range of  $1.519\text{--}1.572 \text{ \AA}$  according to the experimental data [27] and in the range of  $1.537\text{--}1.579 \text{ \AA}$  according to the theoretical calculations [11]. The geometry optimization demonstrated that these distances have close values in the positions  $2_{\text{vol}}$  and  $3_{\text{vol}}$  (Table 2). In the other three positions ( $1_{\text{vol}}$ ,  $4_{\text{vol}}$ ,  $5_{\text{vol}}$ ), the hydrogen atom after the geometry optimization is located either too closely to the nickel atom or too far away from it, which adversely affects the energy of the system. This fact can be explained by the presence of repulsion/attraction forces acting on the H atom from the side of the Mg or Ni atoms located in other layers of the lattice. Thus, we can conclude that the aforementioned positions are metastable and have no significant effect on the hydrogen distribution in the system.

**Table 1.** Lattice parameters ( $\text{\AA}$ ) of the  $\text{Mg}_2\text{Ni}$  compound

References	$a$	$b$	$c$
This work	5.125	5.125	13.026
[10]	5.205	5.205	13.236

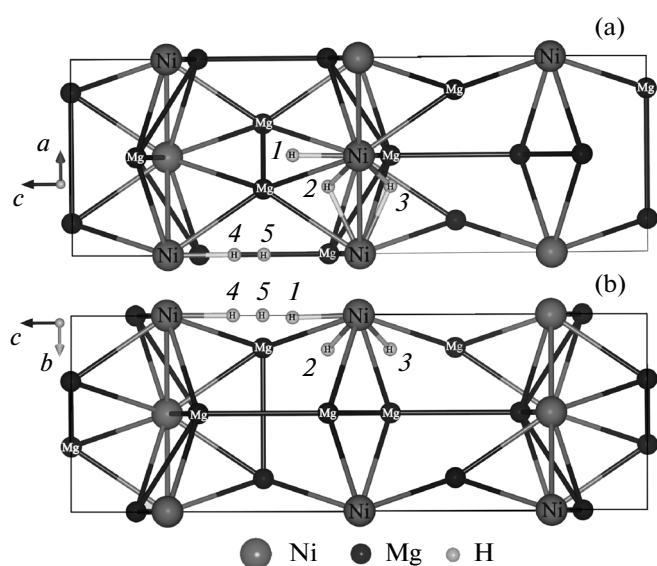


**Fig. 2.** Sorption positions of the hydrogen atom in the  $\text{Mg}_2\text{Ni}$  intermetallic compound: (a) view from the [010] direction and (b) view from the [100] direction.

For a more detailed analysis of the processes occurring in the  $\text{Mg}_2\text{Ni}$  intermetallic compound as it is filled with hydrogen, we considered structures with two and four H atoms located in the most energetically favorable positions  $2_{\text{vol}}$  and  $3_{\text{vol}}$  (Table 3, Fig. 3). In the case of two H atoms in the system, all the considered states are energetically stable, except for the (2d, 3d) configuration where the hydrogen atoms are most closely located to each other at a distance of 1.776 Å. Similarly, the (2b, 3d) configuration has a high energy (the H–H distance is 1.811 Å). The most energetically favorable is the (2a, 2c) structure in which the hydrogen atoms occupy inverted bridge positions with respect to the bond between two atoms in the nickel chain. Since these two atoms occupy the  $2_{\text{vol}}$  positions, the considered state is also stabilized by the energy of Coulomb attraction to the Mg atoms surrounding the nickel chain. Taking into account that the formation energy in this configuration is substantially less than that of a single hydrogen atom, we can conclude that the formation of pair complexes is preferable at suffi-

**Table 2.** Formation energies  $E$  of the compounds per hydrogen atom and the Ni–H distances  $d_{\text{Ni-H}}$  for different sorption positions of hydrogen atoms in the  $\text{Mg}_2\text{Ni}$  supercell

Hydrogen position	$E$ , eV	$d_{\text{Ni-H}}$ , Å
$1_{\text{vol}}$	0.371	1.512
$2_{\text{vol}}$	−0.109	1.582
$3_{\text{vol}}$	−0.104	1.584
$4_{\text{vol}}$	0.406	1.498
$5_{\text{vol}}$	0.601	1.825

cient concentration of the sorbed hydrogen. The calculations demonstrated that the other structures are also stable. Hence, it seems likely that they will arise as intermediate states during the migration of hydrogen atoms with increasing hydrogen concentration. In the energetically favorable structures of  $\text{Mg}_{108}\text{Ni}_{54}\text{H}_2$ , the H–Ni–H bond angles are close both to the experimental data (103.4° and 119.3°) [28] and to the previously obtained theoretical values (107.8° and 111.3°) [11] for the  $\text{Mg}_2\text{NiH}_4$  hydride.

For the structure with four sorbed hydrogen atoms, we calculated three configurations in which these atoms were located far enough away from each other and formed a nearly tetrahedral configuration (Table 3). It should be noted that the formation energy of the considered systems of  $\text{Mg}_{108}\text{Ni}_{54}\text{H}_4$  essentially depends on the structure of the system. For example, despite the energy stability of the positions (3a, 3d), (3a, 3b), and (3b, 3d) in the case of two H atoms, the  $\text{Mg}_{108}\text{Ni}_{54}\text{H}_4$  structure with the hydrogen atoms simultaneously located in the positions (3a, 3b, 3c, 3d) is unstable. This can be explained by the fact that, during the geometry optimization, some H atoms approach each other so that they are separated by short distances (1.82–1.86 Å). In this case, the H–Ni–H bond angles take values far from optimal. A similar situation is observed for the (2a, 2d, 3c, 3b) configuration. Among the calculated configurations, the most energetically favorable is the (2a, 2b, 2c, 2d) configuration, where the additional stability is caused by the stabilizing effect of magnesium atoms (as noted above, the H atoms in the  $2_{\text{vol}}$  positions are located close to Mg).

Further, we analyzed the diffusion of atomic hydrogen in  $\text{Mg}_2\text{Ni}$  in the limit of a low concentration contained in the material at the initial stage of hydrogenation of the intermetallic compound.

We considered several possible migration paths of a single H atom in the  $\text{Mg}_{108}\text{Ni}_{54}$  supercell (Table 4). In the first type of transitions, we simulated a hopping of a hydrogen atom near one Ni atom between different nonequivalent positions ( $4_{\text{vol}}-3_{\text{vol}}$  and  $1_{\text{vol}}-3_{\text{vol}}$ ). In the second type of transitions, we considered the motion of a hydrogen atoms between the most energetically favorable positions: in the first case, it moves from one side of the nickel plane toward the other side (3a–2a); in the second case, it moves in this plane and crosses the chain of nickel atoms; and in the third case, it moves along this chain (3b–2a). In the third type of transitions, the hydrogen atom moves between the  $3_{\text{vol}}$  positions located near the Ni atoms of different layers ( $3_{\text{vol\_Ni1 layer}}-3_{\text{vol\_Ni2 layer}}$ ). In the latter case, it should be noted that the migration of the hydrogen atom between the most energetically favorable positions  $2_{\text{vol}}$  from different planes is hindered, because, in this case, the Mg atom is on the migration path. Therefore, in order to elucidate the possibility of migrating a single atom between different planes, we considered its

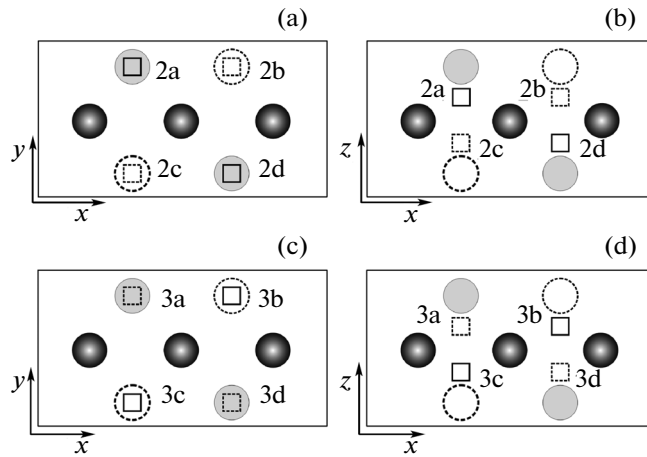


**Fig. 3.** Schematic diagram of sorption positions of the hydrogen atom in  $\text{Mg}_{108}\text{Ni}_{54}\text{H}_2$ : (a) view from the [001] direction for position 2, (b) view from the [010] direction for position 2, (c) view from the [001] direction for position 3, and (d) view from the [010] direction for position 3. Gray spheres are Ni atoms, squares are H atoms, and circles are Mg atoms. Dotted and solid lines indicate atoms in layers located below and above the nickel layer, respectively.

motion by means of successive transitions through several possible intermediate states (the presumed variants of the reaction paths through a set of configurations are as follows:  $2_{\text{vol}}-3_{\text{vol}}-4_{\text{vol}}-3_{\text{vol}}-2_{\text{vol}}$ ;  $2_{\text{vol}}-3_{\text{vol}}-1_{\text{vol}}-3_{\text{vol}}-2_{\text{vol}}$ ; and  $2_{\text{vol}}-3_{\text{vol}}-3_{\text{vol}}-2_{\text{vol}}$ ).

According to the performed calculations, the potential barriers to migration of a single hydrogen atom in the bulk of  $\text{Mg}_2\text{Ni}$  are relatively small. The highest heights ( $\sim 0.6$  eV) are observed for potential barriers corresponding to transitions from the most energetically favorable state  $3_{\text{vol}}$  to the higher energy positions  $4_{\text{vol}}$  and  $1_{\text{vol}}$ . However, when considering the hydrogen diffusion in the material, these states can be excluded from the trajectory of the motion of a single hydrogen atom, because they are not the key positions on the migration path ( $2_{\text{vol}}-3_{\text{vol}}-3_{\text{vol}}-2_{\text{vol}}$ ). Thus, the most important are the transitions along the chain of nickel atoms or between the chains for which the potential barrier heights do not exceed 0.33 eV. Taking into account the low height of these barriers, we can assume that a single hydrogen atom should freely move in the bulk of  $\text{Mg}_2\text{Ni}$ .

The next stage of our investigation was to simulate the behavior of a single hydrogen atom on the surface of  $\text{Mg}_2\text{Ni}$  (the  $\text{Mg}_{126}\text{Ni}_{54}$ (001) plate) and in subsurface layers (Fig. 4). The positions  $4_{\text{surf}}$  and  $5_{\text{surf}}$  differ in that they are located above the nonequivalent nickel atoms,  $1_{\text{surf}}$  corresponds to the position above the second magnesium layer, and  $3_{\text{surf}}$  corresponds to the position above the third magnesium layer. In addition, we performed calculations for another initial arrangement of hydrogen atoms on the surface; however, during the geometry optimization, they moved into any of the positions indicated in Fig. 4. According to the obtained results, the most energetically favorable sorption position is the  $3_{\text{surf}}$  position (Table 5).

It should be noted that, in the case when the hydrogen atoms are located near the nickel atoms situated closer to the surface, the  $2_{\text{vol}}$  position in the bulk of  $\text{Mg}_2\text{Ni}$  becomes more stable as compared to the corresponding state in the bulk of the material ( $-0.415$  and  $-0.109$  eV, respectively). This configuration is also energetically more favorable than the  $3_{\text{surf}}$  position. Consequently, a transition of hydrogen from the surface to subsurface layers is possible.

This assumption was verified by simulating transitions of the H atom over the (001) surface and into subsurface layers. As can be seen from Table 6, the

**Table 3.** Formation energies  $E$  of the compounds per hydrogen atom, the Ni–H distances  $d_{\text{Ni-H}}$ , and the H–Ni–H bond angles  $\varphi$  for different sorption positions of two and four hydrogen atoms in the  $\text{Mg}_2\text{Ni}$  supercell

Hydrogen positions	$E$ , eV	$d_{\text{Ni-H}}$ , Å	$\varphi$ , deg
2a, 2c	-0.714	2.057	77.5, 78.0
2c, 2b	-0.177	3.082	153.2
2c, 2d	-0.182	2.694	115.5
3a, 3b	-0.185	2.639	111.9
3a, 3d	-0.453	2.744	119.0
2d, 3d	0.028	1.776	64.8, 64.9
3b, 3d	-0.138	2.083	78.6, 78.8
2b, 3d	-0.002	1.810	66.8, 66.9
2c, 3d	-0.185	2.653	111.9
2c, 3b	-0.178	3.123	159.3
2a, 2b, 2c, 2d	-0.148	2.110, 2.656	148.3, 108.4, 80.3
3a, 3b, 3c, 3d	0.074	1.817, 2.665	154.2, 115.9, 69.9
2a, 2d, 3c, 3b	0.009	1.8652, 2.5744	154.1, 105.3, 61.6

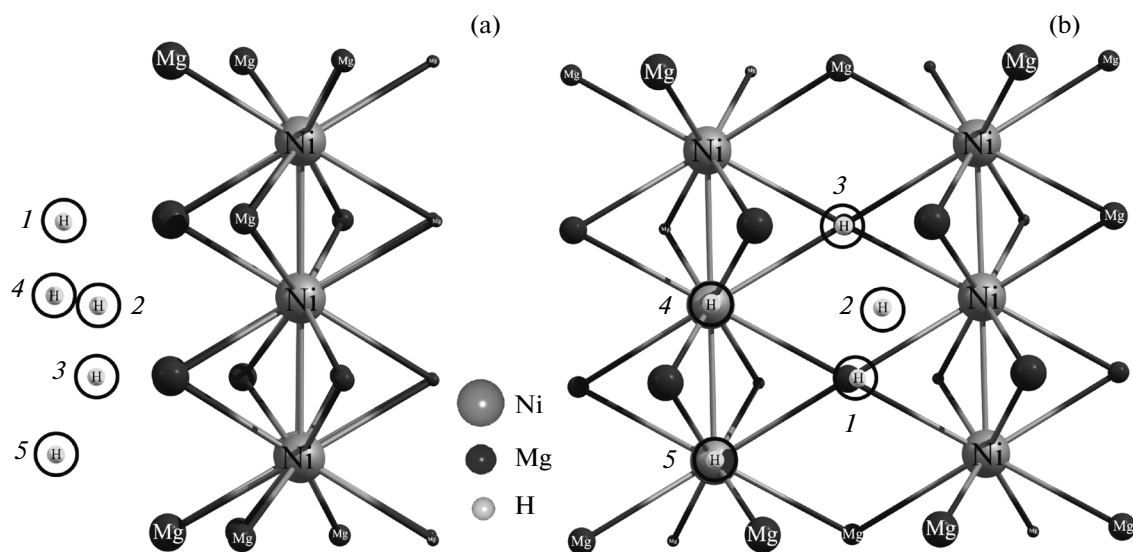


**Fig. 4.** Sorption positions of the hydrogen atom on the surface of the  $\text{Mg}_2\text{Ni}$  intermetallic compound: (a) view from the  $[100]$  direction and (b) view from the  $[001]$  direction.

potential barriers to these transitions are relatively small. Among them, the highest barrier is 0.47 eV. Consequently, the hydrogen atom almost freely moves over the surface of the material. The migration of the hydrogen into the bulk of the material is also not hin-

**Table 4.** Potential barriers to transitions (eV) of the hydrogen atom in the bulk of the  $\text{Mg}_2\text{Ni}$  supercell for different hydrogen migration paths

Initial and final hydrogen positions	Forward direction	Reverse direction
$4_{\text{vol}}-3_{\text{vol}}$	0.08	0.59
$1_{\text{vol}}-3_{\text{vol}}$	0.03	0.51
$3\text{a}-2\text{a}$	0.02	0.03
$3\text{a}-2\text{c}$	0.05	0.05
$3\text{b}-2\text{a}$	0.33	0.33
$3_{\text{vol}}\text{Ni}_1\text{ layer}-3_{\text{vol}}\text{Ni}_2\text{ layer}$	0.31	0.31

**Table 5.** Formation energies  $E$  of the compounds per hydrogen atom and the  $\text{Mg}-\text{H}$  distances  $d_{\text{Mg}-\text{H}}$  for different hydrogen sorption positions on the surface and in subsurface layers of the  $\text{Mg}_{126}\text{Ni}_{54}(001)$  plate

Hydrogen position	$E$ , eV	$d_{\text{Mg}-\text{H}}$ , Å
$1_{\text{surf}}$	0.398	1.928
$2_{\text{surf}}$	-0.069	1.911
$3_{\text{surf}}$	-0.315	1.878
$4_{\text{surf}}$	-0.199	1.896
$5_{\text{surf}}$	-0.188	1.898
$2_{\text{vol}}$	-0.415	1.604

dered, as indicated by the low potential barriers to the transitions  $2_{\text{surf}}-2_{\text{vol}}$  and  $5_{\text{surf}}-2_{\text{vol}}$  ( $\sim 0.3$  eV). These barriers to transitions in the forward direction are significantly lower than those in the reverse direction (0.65 and 0.53 eV, respectively). Thus, in the case of dissociation of  $\text{H}_2$  molecules on the  $\text{Mg}_2\text{Ni}(001)$  surface, the hydrogen atoms should migrate into the bulk of the intermetallic compound.

At the next stage of the work, we considered the sorption of the hydrogen molecule on the (001) surface of  $\text{Mg}_2\text{Ni}$  (Fig. 5). The simulation was performed on the above-described plate of  $\text{Mg}_{126}\text{Ni}_{54}$ . Table 7 presents the results of the calculation of the formation energy and geometric characteristics of the obtained compounds for the cases of the most energetically favorable position of  $\text{H}_2$ . In other cases, the hydrogen molecule during the geometry optimization either passed into these positions or was split into atoms whose energy of bonding to the  $\text{Mg}_2\text{Ni}$  surface proved to be positive. The relatively small values of the formation energy (a few hundredths of electron-volts), large distance between the  $\text{H}_2$  molecules and the nearest surface atoms, and small changes in the  $\text{H}-\text{H}$  bond length in comparison with the equilibrium distance in the gas molecule (0.742 Å) indicate the van der Waals nature of the molecular sorption and the absence of a pre-dissociation complex in the considered system. Consequently, the hydrogen molecules should relatively freely move over the surface of the intermetallic compound, so that their further dissociation can occur from any sorption position.

At the final stage of this work, we investigated different paths of dissociation of the  $\text{H}_2$  molecule as it approached the  $\text{Mg}_2\text{Ni}(001)$  surface. These processes

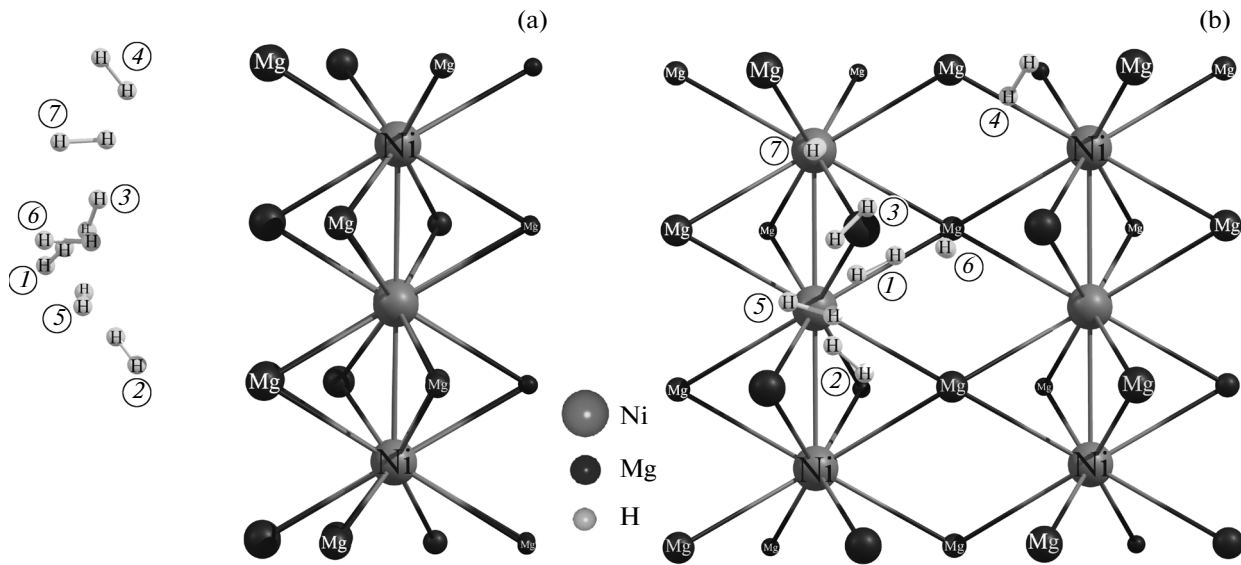


**Fig. 5.** Sorption positions of the hydrogen molecule on the surface of the  $\text{Mg}_2\text{Ni}$  intermetallic compound: (a) view from the  $[100]$  direction and (b) view from the  $[001]$  direction.

were considered as transitions from any stable state of the hydrogen molecule on the surface into two nearest stable atomic positions.

The potential barriers to dissociation of the  $\text{H}_2$  molecule from different positions on the  $\text{Mg}_2\text{Ni}(001)$  surface (Table 8) are less than those in the case of pure magnesium (which, according to [27], is equal to 1.27 eV). In this case, the potential barrier to dissociation from the sorption molecular position  $4_{\text{mol}}$  to the atomic positions  $2_{\text{surf}}$  and  $5_{\text{surf}}$  is 0.43 eV. Hence, it follows that the hydrogen molecules moving over the surface from one sorption molecular position to another position will find themselves in the most favorable situations for the dissociation. Thus, the use of the  $\text{Mg}_2\text{Ni}$  intermetallic compound, for example, in composite magnesium materials will significantly improve the kinetics of hydrogen sorption. However, the potential barriers to hydrogen desorption from the surface in

this case are sufficiently high (0.84–1.30 eV), so that they slow down the desorption process. Therefore, the improvement of the desorption kinetics of hydrogen molecules requires further modification of the surface of magnesium materials.

#### 4. CONCLUSIONS

The most energetically favorable adsorption sites of hydrogen atoms in bulk intermetallic  $\text{Mg}_2\text{Ni}$  have been determined using the DFT calculations. The binding energies of hydrogen atoms within the set of  $\text{Mg}_2\text{NiH}_x$  systems have been calculated. The investigation of the diffusion of single hydrogen atoms in the bulk of the intermetallic  $\text{Mg}_2\text{Ni}$  alloy has demonstrated that the potential barriers to migration are very

**Table 6.** Potential barriers to transitions (eV) of the hydrogen atom over the surface and into subsurface layers of the  $\text{Mg}_{126}\text{Ni}_{54}(001)$  plate for different hydrogen migration paths

Initial and final hydrogen positions	Forward direction	Reverse direction
$2_{\text{surf}}-3_{\text{surf}}$	0	0.24
$2_{\text{surf}}-4_{\text{surf}}$	0.08	0.21
$2_{\text{surf}}-5_{\text{surf}}$	0.03	0.17
$3_{\text{surf}}-5_{\text{surf}}$	0.47	0.35
$2_{\text{surf}}-2_{\text{vol}}$	0.3	0.65
$5_{\text{surf}}-2_{\text{vol}}$	0.29	0.53

**Table 7.** Formation energies  $E$  of the compounds per hydrogen atom, the distances  $d$  from the  $\text{H}_2$  molecule to the surface of the  $\text{Mg}_{126}\text{Ni}_{54}(001)$  plate, and the H–H distances  $d_{\text{H-H}}$  inside the  $\text{H}_2$  molecule for different hydrogen sorption positions on the  $\text{Mg}_{126}\text{Ni}_{54}(001)$  surface

Position of the hydrogen molecule		$E$ , eV	$d$ , Å	$d_{\text{H-H}}$ , Å
Horizontal	$1_{\text{mol}}$	−0.073	3.262	0.752
	$2_{\text{mol}}$	−0.025	2.073	0.759
	$3_{\text{mol}}$	−0.061	2.736	0.755
	$4_{\text{mol}}$	−0.043	2.294	0.756
	$5_{\text{mol}}$	−0.023	2.211	0.761
Vertical	$6_{\text{mol}}$	−0.069	2.826	0.756
	$7_{\text{mol}}$	−0.067	2.626	0.756

**Table 8.** Potential barriers (eV) to dissociative sorption (DS) and associative desorption (AD) of the H<sub>2</sub> molecule for different hydrogen migration paths

Initial position of H <sub>2</sub> molecule—final positions of H atoms	DS	AD
3 <sub>mol</sub> –2 <sub>surf</sub> , 4 <sub>surf</sub>	1.09	1.30
4 <sub>mol</sub> –2 <sub>surf</sub> , 5 <sub>surf</sub>	0.43	0.84
5 <sub>mol</sub> –2 <sub>surf</sub> , 2 <sub>surf</sub>	0.92	1.00
6 <sub>mol</sub> –4 <sub>surf</sub> , 3 <sub>surf</sub>	0.67	1.11
6 <sub>mol</sub> –4 <sub>surf</sub> , 3 <sub>surf</sub>	0.87	1.30
1 <sub>mol</sub> –4 <sub>surf</sub> , 3 <sub>surf</sub>	0.71	1.14

small, which indicates the possibility of free migration of atoms occurring in the structure of this compound. The simulation of sorption processes on the (001) surface has revealed that, at the initial stage of the hydrogen filling (in the case of low hydrogen concentration), the dissociative chemisorption followed by migration of hydrogen atoms into subsurface layers of the material occurs rather easily. However, the desorption from the surface of the intermetallic compound is hindered. Taking into account the thermodynamic and kinetic factors, we can conclude that this compound is promising as a material for hydrogen storage in the case where the surface is modified to facilitate hydrogen desorption.

#### ACKNOWLEDGMENTS

We are grateful to the Institute of Computational Modeling of the Siberian Branch of the Russian Academy of Sciences (Krasnoyarsk, Russia), the Joint Supercomputer Center of the Russian Academy of Sciences (Moscow), the Computer Center of the Siberian Federal University, and the Laboratory of Parallel Information Technologies (SKIF MSU Chebyshev supercomputer) at the Research Computing Center of the Moscow State University [28] for providing an opportunity to use computational clusters for our calculations.

#### REFERENCES

- G. J. Sandrock, *J. Alloys Compd.* **293–295**, 877 (1999).
- K. N. Semenenko, V. N. Verbetskii, and A. V. Kochukov, *Dokl. Akad. Nauk SSSR* **258**, 362 (1981).
- V. N. Verbetskii and S. V. Mitrokhin, *Al'tern. Energy. Ekol.* **10**, 41 (2005).
- E. Ronnebro and D. Noréus, *J. Alloys Compd.* **228**, 115 (2004).
- P. Dantzer, in *Hydrogen in Metals III: Properties and Applications (Topics in Applied Physics: Book 73)*, Ed. by H. Wipf (Springer-Verlag, Berlin, 1997), p. 279.
- M. Gupta and L. Schlapbach, in *Hydrogen in Intermetallic Compounds I: Electronic, Thermodynamic, and Crystallographic Properties, Preparation (Topics in Applied Physics: Book 63)*, Ed. by L. Schlapbach (Springer-Verlag, Berlin, 1988), p. 139.
- J. J. Reilly and R. H. Wiswall, *Inorg. Chem.* **7**, 2254 (1968).
- K. Yvon, J. Schefer, and F. Stucki, *Inorg. Chem.* **20**, 2776 (1981).
- M. Gupta and Esther Belin, *J. Less-Common Met.* **103**, 389 (1984).
- P. Zolliker, K. Yvon, J. D. Jorgensen, and F. Rotella, *Inorg. Chem.* **25**, 3590 (1986).
- W. R. Myers, L.-W. Wang, T. J. Richardson, and M. D. Rubin, *J. Appl. Phys.* **91** (8), 4879 (2002).
- U. Häussermann, H. Blomqvist, and D. Noréus, *Inorg. Chem.* **41** (14), 3684 (2002).
- P. V. Jasen, E. A. González, G. Brizuela, O. A. Nagel, G. A. González, and A. Juan, *Hydrogen Energy* **32**, 4943 (2007).
- J. Zhang, D. W. Zhou, and L. P. He, and J. S. Lui, *J. Phys. Chem. Solids* **70** (1), 32 (2009).
- A. Zütte, *Mater. Today* **9**, 24 (2003).
- G. Kresse and J. Hafner, *Phys. Rev. B: Condens. Matter* **47**, 558 (1993).
- G. Kresse and J. Hafner, *Phys. Rev. B: Condens. Matter* **49**, 14251 (1994).
- G. Kresse and J. Furthmüller, *Phys. Rev. B: Condens. Matter* **54**, 11169 (1996).
- P. Hohenberg and W. Kohn, *Phys. Rev.* **136**, 864 (1964).
- W. Kohn, *Phys. Rev.* **140**, 1133 (1965).
- P. E. Blöchl, *Phys. Rev. B: Condens. Matter* **50**, 17953 (1994).
- G. Kresse and J. Joubert, *Phys. Rev. B: Condens. Matter* **59**, 1758 (1999).
- S. Grimme, *J. Comput. Chem.* **27**, 1787 (2006).
- G. Henkelman, B. P. Uberuaga, and H. Jónsson, *J. Chem. Phys.* **113**, 9901 (2000).
- G. Henkelman and H. Jónsson, *J. Chem. Phys.* **113**, 9978 (2000).
- H. J. Monkhorst and J. D. Pack, *Phys. Rev. B: Solid State* **13**, 5188 (1976).
- J. L. Soubeyroux, D. Fruchart, and A. Mikou, *Mater. Res. Bull.* **19**, 895 (1984).
- K. Yvon, *Chimia* **10** (10), 613 (1998).
- A. S. Fedorov, M. V. Serzhantova, and A. A. Kuzubov, *J. Exp. Theor. Phys.* **107** (1), 126 (2008).
- V. V. Voevodin, S. A. Zhumatii, S. I. Sobolev, A. Antonov, P. Bryzgalov, D. Nikitenko, and K. Stefanov, *Practice of "Lomonosov" Supercomputer* (Open Systems, Moscow, 2012), p. 7 [in Russian].

Translated by O. Borovik-Romanova